

Published in final edited form as:

Biomaterials. 2010 May ; 31(13): 3736–3743. doi:10.1016/j.biomaterials.2010.01.058.

Bioactive Hydrogels Made from Step-Growth Derived PEG-Peptide Macromers

Jordan S. Miller, Colette J. Shen, Wesley R. Legant, Jan D. Baranski, Brandon L. Blakely, and Christopher S. Chen*

University of Pennsylvania, Department of Bioengineering, 210 S. 33rd St., 510 Skirkanich Hall, Philadelphia, PA 19104

Abstract

Synthetic hydrogels based on poly(ethylene glycol) (PEG) have been used as biomaterials for cell biology and tissue engineering investigations. Bioactive PEG-based gels have largely relied on heterobifunctional or multi-arm PEG precursors that can be difficult to synthesize and characterize or expensive to obtain. Here, we report an alternative strategy, which instead uses inexpensive and readily available PEG precursors to simplify reactant sourcing. This new approach provides a robust system in which to probe cellular interactions with the microenvironment. We used the step-growth polymerization of PEG diacrylate (PEGDA, 3400 Da) with bis-cysteine matrix metalloproteinase (MMP)-sensitive peptides via Michael-type addition to form biodegradable photoactive macromers of the form acrylate-PEG-(peptide-PEG)_m-acrylate. The molecular weight (MW) of these macromers is controlled by the stoichiometry of the reaction, with a high proportion of resultant macromer species greater than 500 kDa. In addition, the polydispersity of these materials was nearly identical for three different MMP-sensitive peptide sequences subjected to the same reaction conditions. When photopolymerized into hydrogels, these high MW materials exhibit increased swelling and sensitivity to collagenase-mediated degradation as compared to previously published PEG hydrogel systems. Cell-adhesive acrylate-PEG-CGRGDS was synthesized similarly and its immobilization and stability in solid hydrogels was characterized with a modified Lowry assay. To illustrate the functional utility of this approach in a biological setting, we applied this system to develop materials that promote angiogenesis in an *ex vivo* aortic arch explant assay. We demonstrate the formation and invasion of new sprouts mediated by endothelial cells into the hydrogels from embedded embryonic chick aortic arches. Furthermore, we show that this capillary sprouting and three-dimensional migration of endothelial cells can be tuned by engineering the MMP-susceptibility of the hydrogels and the presence of functional immobilized adhesive ligands (CGRGDS vs. CGRGES peptide). The facile chemistry described and significant cellular responses observed suggest the usefulness of these materials in a variety of *in vitro* and *ex vivo* biologic investigations, and may aid in the design or refinement of material systems for a range of tissue engineering approaches.

Introduction

In the past several decades, engineered materials have become an increasingly important and versatile tool for mimicking the native *in vivo* environment, and provide unparalleled control over the cellular microenvironment compared to the substantially more complex naturally-

*Correspondence: chrischen@seas.upenn.edu.

Publisher's Disclaimer: This is a PDF file of an unedited manuscript that has been accepted for publication. As a service to our customers we are providing this early version of the manuscript. The manuscript will undergo copyediting, typesetting, and review of the resulting proof before it is published in its final citable form. Please note that during the production process errors may be discovered which could affect the content, and all legal disclaimers that apply to the journal pertain.

derived materials [1]. Hydrogels, owing to their hydrophilic nature and ability to absorb large amounts of water, are one class of materials that have received significant attention for cell biology and tissue engineering applications [2]. A widely investigated class of synthetic hydrogels is based on poly(ethylene glycol) (PEG), whose neutral charge, hydrophilicity, and resistance to protein adsorption make them biocompatible for both *in vitro* and *in vivo* experiments, as well as an attractive platform for synthetic chemistry [3–10]. While PEG alone is unable to support cellular activity, copolymers of PEG and biologically active moieties including peptides have been successfully applied in a diverse range of *in vitro* and *in vivo* studies. From a design perspective, the peptides or proteins conjugated to PEG are the main controls used to engineer the bioactive and bioresponsive character of these synthetic gels. PEG-peptide hydrogels have been utilized in the three-dimensional study of ensemble fibroblast migration [11–13], chondrocyte maintenance for cartilage engineering [14,15], hepatocyte metabolism [16], valvular interstitial cell matrix secretion [17], and a range of other applications [18–20].

A variety of coupling chemistries and hydrogel architectures have been used, ultimately imparting PEG hydrogels with similar properties that are attractive in these diverse biomedical applications. West and Hubbell developed early hydrogels sensitive to the activity of matrix metalloproteinases (MMPs) made of block copolymers of degradable peptides and PEG, flanked with photopolymerizable acrylates [4]. Later innovations by West and colleagues led to hydrogel redesign by reacting heterobifunctional acrylate-PEG-N-hydroxysuccinimide active esters with bis-amine MMP-sensitive peptides to form precursors of the form acrylate-PEG-peptide-PEG-acrylate [21,11]. Hubbell and colleagues also introduced an approach using Michael-type addition between bis-cysteine MMP-sensitive peptides and 4-arm PEG-vinylsulfones to cross-link reactants into a hydrogel in a single step [5,7]. Similarly, Anseth and colleagues have utilized multi-arm PEGs in thiol-ene photopolymerization [22] and novel click-chemistries [23] to tailor the cellular microenvironment.

These bioactive PEG-based hydrogels are being explored as a scaffolding to support tissue engineering. Because these materials ultimately will be implanted *in vivo* to support thick multicellular constructs, the ability of such hydrogels to support angiogenesis—the physiologic sprouting of new blood vessels from existing ones—and vascular integration of an implant also will need to be optimized. Although angiogenesis has been extensively studied in natural materials such as collagen and fibrin gels [24,25], or Matrigel [26], investigators are only just beginning to examine how to engineer PEG-based hydrogels to support vascular ingrowth. Recent studies have shown promise via the encapsulation or immobilization of vascular endothelial growth factor (VEGF) [27–29] or Ephrin-A1 [30] in these materials.

Here, we report an approach to generate PEG-based hydrogels that appear to support rapid vascular invasion. In the first stage of synthesis, we used the step-growth polymerization of bis-cysteine MMP-sensitive peptides and PEG-diacrylate (PEGDA) to make high molecular weight (MW) photoactive macromers. These macromers were then crosslinked into hydrogels during a second radical-mediated photopolymerization step. Resultant hydrogels were further characterized for MMP-susceptibility and the ability to support cell adhesion, and then assessed for angiogenic potential with an *ex vivo* chick aortic arch assay. The synthetic approach presented here highlights the potential utility of PEG-based hydrogels to support and control angiogenesis.

Materials and Methods

Reagents and Cell Maintenance

All reagents were from Sigma-Aldrich (St. Louis, MO) and were used as received unless otherwise described. Acryloyl chloride was from Alfa Aesar (Ward Hill, MA). Culture media

and human umbilical vein endothelial cells (HUVECs) were from Lonza (Basel, Switzerland), and were maintained in complete Endothelial Growth Medium-2 (EGM-2, Lonza).

Synthesis and Characterization of Poly(ethylene glycol) Diacrylate (PEGDA)

Dry poly(ethylene glycol) (PEG; MW 3400 or 6000) was acrylated by reaction with triethylamine (TEA; clear, colorless, 2 molar excess to PEG) and acryloyl chloride (clear, colorless, 4 molar excess to PEG) in anhydrous dichloromethane under argon as described previously [21]. Yields were typically in the range 80–90% (~120 g), and percent acrylation was 99% as verified by ^1H NMR for the characteristic peak (4.32 ppm) of the PEG methylene protons adjacent to the acrylate [21].

Synthesis of MMP-sensitive acrylate-PEG-(peptide-PEG)_m-acrylate Conjugates

The bis-cysteine peptide sequences CGPQGIWGQGCR (highly degradable, HD, 1261.42 g/mol), CGPQGIAGQGCR (native collagen, NC, 1146.28 g/mol), and CGPQGPAGQGCR (least degradable, LD, 1130.23 g/mol) were custom synthesized by Aapptec (Louisville, KY). Each peptide was supplied as a trifluoroacetate salt at >95% purity. Peptides were evacuated of air and stored under argon (to minimize disulfide formation) at -80°C until needed. In a typical reaction, 183.8 μmol bis-cysteine peptide (HD, 231.6 mg) was reacted with a 1.6 molar excess of PEGDA (3400 Da, 1 g, 294.1 μmol) by dissolution in 10 mL 100 mM sodium phosphate, pH 8.0 (94.7 mM Na_2HPO_4 , 5.3 mM NaH_2PO_4). The reaction was sterile filtered through a 0.22 μm PVDF membrane (Millipore, Billerica, MA), protected from light and proceeded on a circular shaker for 85 hr at room temperature to yield acrylate-PEG-(peptide-PEG)_m-acrylate conjugates. The reaction mixture was dialyzed against 4 L 18 M Ω water (Millipore) with pre-swollen regenerated cellulose dialysis tubing (MWCO 3500, “snake-skin”, Pierce, Rockford, IL) for 24 hr (4 water changes). The dialyzed PEG-peptide conjugates were frozen overnight (-20°C), lyophilized, and stored at -80°C until use.

Characterization of PEG-Peptide Macromers by GPC

PEG-peptide conjugates were analyzed by GPC with a refractive index detector and DMF solvent using three tandem styrene-divinylbenzene (SDVB) columns spanning a linear MW range from 1 kDa to 500 kDa for polystyrene. PEG MW standards from 628 Da to 478 kDa (Sigma) were used for assessment of the molecular weight of the PEG-peptide conjugates.

PEG-Peptide Macromer Photopolymerization to form Hydrogels

PEGDA or PEG-peptide macromers were individually dissolved at 8–20% w/w concentration in PBS to make stock prepolymer solutions at the beginning of each experiment. The desired amounts of cell-adhesive and MMP-sensitive macromers were then mixed and diluted to the proper experimental concentration with PBS. To maintain concentration accuracy during dissolution, it was noted that PBS volume increased upon addition of PEG-peptide conjugates by approximately 0.9 $\mu\text{L}/\text{mg}$ added. **All macromers are reported as their initial concentration during hydrogel polymerization.** A solution (100 mg/mL in 100% ethanol) of the photoinitiator Irgacure 2959 (I2959, Ciba, Tarrytown, NY), was added to a final working concentration of 0.05% w/v (by using 5 μL of the initiator solution per 1 mL hydrogel prepolymer solution). Solutions were thoroughly mixed and sonicated before polymerization. The prepolymer solution was transferred into plastic molds (96-well plate) for degradation assays, between glass plates for the modified Lowry assay, or dispensed onto a sterile slab of poly(dimethyl siloxane) (PDMS; Dow Corning) for explant encapsulation as described below. Photopolymerization was conducted with an Omnicure S2000 (320–500 nm, EXFO, Ontario, Canada) lamp at 100 mW/cm² (measured for 365 nm) to yield solid hydrogels (exposure times reported in relevant sections below). Hydrogels containing explants were easily transferred into culture media with flat, round tip tweezers (EMS, Switzerland).

Characterization of MMP-sensitive PEG-peptide Hydrogels by Collagenase Degradation

A collagenase degradation assay was employed to check the MMP-sensitivity of these hydrogels and their relative degradation behavior, in a similar fashion as described previously [21]. Briefly, hydrogel prepolymer solutions were made in HEPES-buffered saline (HBS; 10 mM, pH 7.4) containing 0.2 mg/mL sodium azide (to inhibit microbial growth), mixed with initiator, and polymerized for 60 sec as described above. Hydrogels (150 μ L starting volume per gel) were swollen for 36 hr at 37 °C and weighed to assess equilibrium swollen weight. These swollen hydrogels were then transferred to a 0.2 mg/mL collagenase solution (made with the same buffer) and their wet weight was monitored over time (3 gels per condition). Control hydrogels were incubated in buffer without enzyme.

Synthesis and Characterization of Cell-adhesive acrylate-PEG-peptide Conjugates

Cell adhesive or non-adhesive acrylate-PEG-peptide conjugates were prepared in a similar manner to the MMP-sensitive conjugates by using a 1.0 molar equivalent of PEGDA 3400 for the monocysteine peptides CGRGDS (adhesive, 593.59 g/mol) and CGRGES (non-adhesive, 607.62 g/mol). These conjugates were characterized by GPC as described above.

Characterization of the Immobilization Stability of Cell-adhesive acrylate-PEG-peptide conjugates

To verify the immobilization stability of acrylate-PEG-RGDS in PEG gels we developed a modified Lowry Assay (Sigma) in prepolymer solutions or in solid hydrogels to quantify peptide concentration *in situ*. For solutions, acrylate-PEG-CGRGDS solutions were made in sterile water (the Lowry assay is not reliable in PBS) and assessed as described below with the free peptide CGREDV used as a standard. For solid hydrogels, 10% w/w PEGDA 6000 hydrogel prepolymer solutions were made containing 0, 0.25, 2, or 4 μ mol/mL acrylate-PEG-CGRGDS. Initiator was added as described above, then each solution was transferred to a glass chamber composed of thin rubber spacers sandwiched between two glass slides (chamber dimensions: 30 mm \times 40 mm \times 0.48 mm thick). Hydrogels were polymerized for 120 seconds (25 mW/cm²) and then sliced into 3 sections to yield hydrogels approximately 7 mm \times 15 mm \times 0.48 mm. Gels were subjected to a modified Lowry assay immediately after polymerization, or after a 24 hr or 72 hr incubation at 37 °C in sterile water (changed daily). At these specified times, hydrogels were blotted dry with laboratory wipes, then placed in a test tube with 1 mL deionized water. While vigorously mixing, 1 mL Lowry reagent was added according to the vendor's recommendations. Mixing continued for 40 sec and hydrogels were left at room temperature for 20 min. While vigorously mixing, 0.5 mL Folin-Ciocalteu's phenol reagent was added. Mixing continued for 40 sec and hydrogels were left at room temperature for 30 min. Hydrogels were blotted dry, transferred to plastic cuvettes and assessed with a UV/Vis spectrophotometer (750 nm) transverse to the wide hydrogel face. Absorbance values were normalized to PEGDA gels without peptide.

Characterization of cell attachment to adhesive acrylate-PEG-peptide conjugates

Cell-adhesive 20% w/w PEGDA 3400 hydrogels were formed containing 4 μ mol/mL acrylate-PEG-CGRGDS or acrylate-PEG-CGRGES in PBS and swollen for 24 hr at 37 °C. Hydrogels were briefly rinsed with media, then seeded with HUVECs (15,000 cells/cm²). Hydrogels were rinsed with PBS after 24 hr and photographed to check cellular attachment.

Chick Aortic Arch Explant Angiogenesis Assay

Chick aortas were isolated from 12-day-old chick embryos (Charles River Labs, Preston, CT). Aortic arches were cleaned of excess fibroadipose tissue, sectioned into ~0.5 mm sized rings, and submerged inside a 30 μ L droplet of hydrogel prepolymer solution (final concentrations of 8% w/w MMP-sensitive and 1.0 μ mol/mL adhesive components). Polymerization was

performed for 30 sec as described above, and culture media (EGM-2; 0.75 mL per hydrogel) was changed on day 1 and every 3 days thereafter. Hydrogels were photographed daily with oblique lighting phase contrast microscopy to optically exclude 2D cell migration on the surface of hydrogels and instead visualize only those cells which migrated in 3D within the hydrogels. Sprout area was assessed by image thresholding and edge-finding filters (Adobe Photoshop, NIH ImageJ), 2 sides per arch ring, 6 arch rings per experimental group. Statistics were assessed by one-way ANOVA with Tukey's HSD post-hoc testing, and p-values less than 0.05 were considered significant. For time-lapse microscopy (Movie1, Supporting Information), hydrogels containing arch pieces were polymerized on round coverslips (22 mm) that were functionalized with 3-(trimethoxysilyl)propyl methacrylate according to the manufacturer's instructions (Sigma) to covalently link the hydrogel to the glass coverslip.

Briefly, coverslips were sonicated in Alconox detergent, rinsed with 18 M Ω water, blown dry with nitrogen, and baked at 110 °C for 30 min. Cleaned and dried coverslips were then placed in a 2% v/v solution of the silane in EtOH (200 mL) with dilute acetic acid (6 mL, 1:10 glacial acetic acid:water) at room temperature for 1 hr, blown dry with nitrogen, then baked at 60 °C for 1 hr. Hydrogel prepolymer solutions (20 μ L) were placed into PDMS wells on these coverslips and photopolymerized as described above. After 2 days in culture, these gels were mounted on an environmentally controlled microscope (5% CO₂, 37 °C; Zeiss Axiovert 200M, Carl Zeiss, Germany) and imaged by oblique lighting phase contrast every hour. For endothelial cell labeling experiments, aortic arches explants were incubated with rhodamine-lectin (Lens culinaris agglutinin, 20 μ g/mL, Vector Laboratories) for 1.5 hr before encapsulation in hydrogels.

Results and Discussion

Macromer Design and Analysis

This work examines the step-growth polymerization of PEGDA with MMP-sensitive peptides for tissue engineering and cell biology applications. We started with synthesis of PEGDA from PEG, as previously described (Figure 1a, [21]). Importantly, ensuring the clear and colorless properties of the starting reagents TEA and acryloyl chloride are critical to achieving a high percentage of acrylation. With pure reagents, this synthesis lends itself well to scale-up in the laboratory, with PEGDA batch yields routinely 120 g or greater (80–90% yield) and percent acrylation greater than 99%. Compared to other routes to bioactive PEG-based hydrogels, which employ acrylate-PEG-NHS [11] or multi-arm PEGs [13, 22], our approach here is much less subject to proprietary restrictions, vendor sourcing or availability issues, or synthetic difficulties. Material cost for the current approach is also dramatically reduced for these simple PEGs (up to 100 \times based on current market rates). Indeed the entire range of readily available PEG molecular weights, from oligoethylene glycols to 100 kDa poly(ethylene oxide) should be amenable to this synthetic scheme. Keeping future *in vivo* targets in mind, PEG 3400 was chosen as the base structural unit for these hydrogels due to its well-known ability to be cleared *in vivo*. As with other synthetic approaches, we believe the current approach to be extremely flexible for examining a wide variety of matrix properties. In this work we examined the effects of hydrogel degradation rate on 3D angiogenic sprouting.

Our strategy employed an initial step-growth polymerization between PEG and peptides to yield soluble, high MW photoactive precursors. MMP-sensitive peptide sequences were selected based on a range of known degradabilities [31], and previous work with this family of sequences in degradable hydrogels [18,32]. These base sequences were flanked with leading and lagging cysteine residues (Figure 1a; HD = highly degradable, CN = collagen native, LD = least degradable) to allow for reaction with the terminal acrylates on PEGDA. Our use of PEGDA rather than multi-arm PEGs means that step-growth polymerization does not result in hydrogel formation directly, but rather leads to macromer chain extension such that multiple

MMP-sensitive peptides are incorporated into each polymer chain (Figure 1b). Sodium phosphate buffer pH 8.0 proved an effective buffer for macromer coupling because it is sufficiently basic to allow for Michael-type addition while still mild enough to leave the terminal ester bonds of PEGDA intact. Furthermore, disulfide bonding is not favored under these conditions [5].

The resulting high MW macromers could then be purified and reconstituted in phosphate buffered saline (PBS), and crosslinked in the presence of living cells to form bioactive hydrogels in a second rapid photopolymerization step (Figure 1b). We found the main characteristics of this unique system to be increased hydrogel swelling and collagenase sensitivity, and dramatically decreased material cost, compared to other synthetic strategies for PEG-based gels.

Step-growth polymerization is strongly controlled by the stoichiometric ratio of the reactants, and we found large differences in resultant polydispersity based on the starting ratio of PEGDA:peptide used for each reaction (Figure 2). In order to ensure that acrylates remained at the terminal ends of MMP-sensitive macromers (to enable later photopolymerization), an excess of PEGDA compared to peptide was used. With a PEGDA:peptide molar ratio of 2.2, more than 80% of the PEGDA reacted with peptide (sum of “high” and “medium” MWs in Figure 2) indicating successful Michael-type addition. Surprisingly, approximately 40% of the resultant molecular species were greater than 500 kDa. Unreacted MMP-sensitive peptide was not observed by GPC, either due to the completeness of the reaction or from being washed away during dialysis.

To achieve higher coupling efficiency, a PEGDA:peptide ratio of 1.6 was used (Figure 2). In this case, more than 90% of the PEGDA reacted with peptide and approximately 60% of the molecular species were greater than 500 kDa. Importantly, all three MMP-sensitive peptides showed nearly identical polydispersity, indicating that Michael-type addition proceeded similarly for each peptide sequence. Reacted species are of the form acrylate-PEG-(peptide-PEG)_m-acrylate, and for a macromer MW of 500 kDa, the m-value is approximately 100.

To make pendant cell-adhesive RGDS peptide, we reacted CGRGDS peptide with PEGDA 3400 under similar conditions but with a PEG:peptide ratio of 1.0. GPC analysis showed that 87% of the PEGDA reacted with peptide. The lack of a second cysteine residue on this peptide prevents step-growth polymerization and thus the possibility of high MW macromers. However, double conjugation in the form peptide-PEG-peptide is possible in this reaction. Of the peptide-conjugated PEGDA, 63% was in the preferred acrylate-PEG-CGRGDS form. These data suggested sufficient coupling of peptide for their covalent incorporation into hydrogels as cell-adhesive pendant chains.

Hydrogel Degradation in Collagenase

Step-growth derived macromers were photopolymerized into hydrogels, which were allowed to reach equilibrium swelling in aqueous buffer and then degraded in 0.2 mg/mL collagenase while their wet-weight was monitored. Buffer without collagenase served as negative control. Hydrogels absorbed a large amount of buffer solution during equilibrium swelling, with 10 wt % gels gaining a factor of 2.5× of their as-polymerized weight (Figure 3a). This compares with a factor of 1.2–1.4× equilibrium swelling weight gain as reported for similar hydrogels [21, 32]. The dramatic equilibrium swelling of these hydrogels is due to the high MW of the macromers in the hydrogel pre-polymer solution. The highly swollen nature of these gels, and the presence of multiple degradable peptides within each macromer chain were likely the principal contributors to their rapid degradation, with all gels fully degrading within 8 hr (Figure 3b). These observed hydrogel degradation profiles differ substantially from the degradabilities reported for these sequences when in soluble form. Relative to the native

collagen sequence (CN), reported degradabilities for HD and LD peptides in solution are 800% and 0.5%, respectively [31]. In contrast, the degradation curves for hydrogels containing HD and CN peptides overlapped nearly identically. This overlap is likely a result of the concentration of collagenase used (0.2 mg/mL) which was selected to be consistent with the literature for these assays. Indeed, angiogenic sprouting assays (described below) indicate a significant difference between the degradable behaviors of these materials. Additionally, LD hydrogels required nearly twice the amount of time to fully degrade in collagenase compared to HD and CN gels. The difference in the reported degradabilities for soluble peptides compared to our observed degradation profiles for solid hydrogels may be attributed to the many repeating degradable peptides in the hydrogel backbone of the form acrylate-PEG-(peptide-PEG)_m-acrylate. Indeed, these hydrogels degrade extremely rapidly in collagenase compared to other MMP-sensitive hydrogels [21].

Quantification of Acrylate-PEG-CGRGDS Immobilization and Assessment of Bioactive Potency

To enable cell-substrate adhesion in these MMP-sensitive hydrogels we employed the well-known RGDS peptide using a similar synthetic approach as that for step-growth polymerization (Figure 1a). To quantify the amount of RGDS entrapped or immobilized in the hydrogel during polymerization and its subsequent stability in the hydrogel over time, we developed a modified Lowry Assay for *in situ* quantification [33]. Using this new modification, we were able to quantify the concentration and stability of immobilized adhesive peptide in hydrogels over time (Figure 4a–d). The Lowry assay provides a colorimetric measurement of the total amount of peptide bonds present and is typically quantified relative to a bovine serum albumin (BSA) control. Because BSA was not a suitable standard for the short peptides employed here, which have comparatively fewer peptide bonds per mg of material, we first established the use of the short peptide CGREDV as a standard, which has the same number of peptide bonds as the peptides used in these experiments. Known amounts of CGREDV peptide were diluted in solution and quantified by Lowry assay. The resulting linear standard curve verified that the Lowry assay, typically used only for large proteins, could be used to quantify the concentration of short peptides (Figure 4a). When this standard curve was applied to our acrylate-PEG-CGRGDS materials diluted in solution, we found an equivalence of peptide measured as expected for starting dry weight of the PEG-peptide conjugate with a deviation from expected of 1.4–1.5× (Figure 4b). We then applied this assay to characterize the immobilization of CGRGDS into solid hydrogels. To remove the potentially confounding influence of degradable peptide immobilized in the gels, this assay was applied to non-degradable PEGDA hydrogels with or without adhesive ligand peptide. In solid hydrogel slabs, we again found a linear relationship between absorbance and peptide amount used (Figure 4c), which validated this modified Lowry assay for solid hydrogels. To estimate the amount of peptide immobilized to the hydrogel, we followed relative peptide retention in hydrogels over time (Figure 4d). In the first day of equilibrium swelling, hydrogels lost between 30–50% of the PEGDA-peptide conjugate. The remaining immobilized peptide was stable in the gel thereafter (Fig 3b). These results are consistent with GPC analysis of the CGRGDS-conjugate, which indicated 63% in the preferred mono-conjugated acrylate-PEG-CGRGDS form. That is, double-conjugated peptide-PEG-peptide would initially be physically entrapped in the gel but would diffuse away during equilibrium swelling within the first day. These data therefore suggest that the preferred acrylate-PEG-CGRGDS species are largely covalently incorporated into the hydrogel. As stated in **Materials and Methods**, all adhesive macromers are reported as their initial concentration during hydrogel polymerization to aid in reproducing the results obtained here and to remain consistent with the existing literature. Moreover, this new modification of the Lowry assay may find uses in other hydrogel systems for verifying peptide immobilization and stability *in situ*.

We next confirmed the bioactive potency of our cell-adhesive conjugate using surface adhesion of human umbilical endothelial cells (HUVECs) to PEGDA hydrogels containing the cell-adhesive CGRGDS or non-adhesive CGRGES peptide (Figure 4e). While negative control CGRGES peptide was unable to support HUVEC adhesion, CGRGDS peptide supported robust HUVEC adhesion and cell spreading. This assay provided an initial check of the bioactivity of our cell-adhesive conjugates, and confirms that sufficient adhesive PEG-peptide is immobilized in the hydrogels to support cell adhesion. Because HUVEC adhesion to PEG-based hydrogels containing RGDS peptide has been studied in detail elsewhere [29, 34], we instead focused on applying these conjugates to support three-dimensional studies of angiogenic sprouting.

Aortic Arch Explant Assay

The possibility of using these materials to observe and control three-dimensional cell migration was examined with the chick aortic arch assay, in which angiogenic sprouting from embryonic chick explants (typically done in fibrin or collagen gels) is a reliable predictor of factors that stimulate angiogenesis *in vivo* [35,36]. While endothelial cells are activated into an angiogenic phenotype by numerous factors such as vascular endothelial growth factor (VEGF) [37], their ability to form new vessels is likely also physically constrained and regulated by the interplay of cell-secreted MMPs with the extracellular matrix [38,39]. To test this possibility, we used each of the three MMP-degradable sequences in our hydrogels to vary only MMP-susceptibility, while holding polymer weight percent and adhesive peptide concentration constant. Dark field imaging through oblique lighting phase contrast microscopy illuminated only cells within 3D angiogenic sprouts, allowing direct imaging and quantitation specifically of 3D sprouting.

Significantly more 3D angiogenic sprouting was observed in the hydrogels containing the most degradable peptide sequences (Figure 5a,b). Representative images demonstrate the character and time course of sprouting into these hydrogels. Quantification of area of sprouting from each explant demonstrates statistical significance between the three different experimental groups ($p < 0.003$ for all comparisons by one-way ANOVA and post-hoc testing). Moreover, angiogenic sprouting was completely suppressed to undetectable levels by substitution of CGRGDS with the non-adhesive CGRGES peptide, confirming that the hydrogels support angiogenic invasion only in the presence of an adhesive peptide. To verify that the observed explant sprouts were of endothelial origin, we incubated the chick arches with rhodamine-conjugated *Lens culinaris agglutinin* lectin, which specifically labels endothelial cells [40]. Indeed, endothelial cells were a principal component of the newly formed sprouts (Figure 5c). Supplemental Movie 1 demonstrates a dark field time-course of angiogenic sprouting in these MMP-sensitive hydrogels. To visualize an angiogenic sprouting time-course in a single image we selected sequential movie frames 12–14 hours apart, false-colored them with time, and then overlaid them with no lateral translation (Figure 5d).

Conclusions

This work describes an inexpensive, flexible, and readily available route to bioactive PEG-based hydrogels, which can modulate *ex vivo* angiogenic sprouting through chemical control of MMP-susceptibility. Step-growth polymerization via Michael-type addition was employed to create high MW bioactive macromers of the form acrylate-PEG-(peptide-PEG)_m-acrylate. Under the conditions described, the synthetic scheme yields polydisperse materials with a majority of molecular species greater than 500 kDa. The presence of terminal acrylate groups permits photopolymerization via standard techniques, and the resultant hydrogels were highly susceptible to collagenase-mediated degradation. A peptide quantification assay was designed and employed to verify the amount of cell-adhesive peptide covalently incorporated into these

hydrogels. These materials were then applied to examine, for the first time, 3D angiogenic sprouting from an *ex vivo* chick aortic arch assay into wholly synthetic materials. Angiogenic sprouts contained endothelial cells, and the sprouting response depended on both the MMP-susceptibility of the hydrogel backbone and the presence of adhesive peptide (CGRGDS compared to CGRGES). The control of angiogenic sprouting demonstrated here through modification of MMP-susceptibility alone highlights the general power of a synthetic approach to isolate a single parameter that in a natural scaffolding cannot be controlled independently from other properties. Specifically, this work may provide a new avenue to promote blood vessel growth in synthetic materials for tissue engineering and cell biology applications.

Supplementary Material

Refer to Web version on PubMed Central for supplementary material.

Acknowledgments

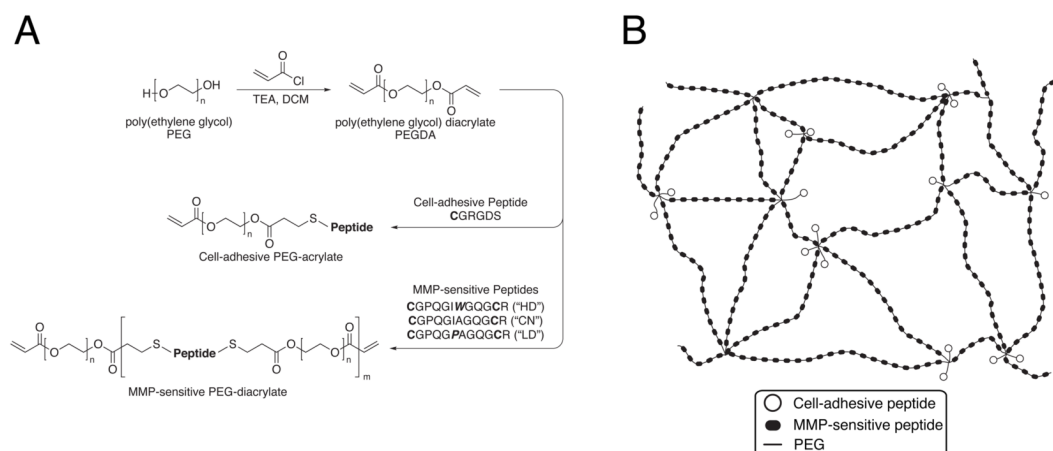
We thank Jeffrey Bode and Shouyun Yu for assistance with GPC. This work was supported by grants from the National Institutes of Health (EB00262, HL73305, GM74048), NIH T32 Training Grant (J.S.M., HL007954) and The Hartwell Foundation (J.S.M.), Ruth L. Kirschstein National Research Service Award (C.J.S., HL095332), NSF Graduate Research Fellowship (W.R.L.), and the DHS Scholarship and Fellowship Program (B.L.B.).

References

1. Lutolf MP, Hubbell JA. Synthetic biomaterials as instructive extracellular microenvironments for morphogenesis in tissue engineering. *Nat Biotechnol* 2005;23:47–55. [PubMed: 15637621]
2. Tibbitt MW, Anseth KS. Hydrogels as extracellular matrix mimics for 3D cell culture. *Biotechnol Bioeng* 2009;103:655–63. [PubMed: 19472329]
3. Hill-West JL, Chowdhury SM, Sawhney AS, Pathak CP, Dunn RC, Hubbell JA. Prevention of postoperative adhesions in the rat by in situ photopolymerization of bioresorbable hydrogel barriers. *Obstet Gynecol* 1994;83:59–64. [PubMed: 8272310]
4. West J, Hubbell J. Polymeric biomaterials with degradation sites for proteases involved in cell migration. *Macromolecules* 1999;32:241–4.
5. Lutolf MP, Hubbell JA. Synthesis and physicochemical characterization of end-linked poly(ethylene glycol)-co-peptide hydrogels formed by Michael-type addition. *Biomacromolecules* 2003;4:713–22. [PubMed: 12741789]
6. Lutolf MP, Lauer-Fields JL, Schmoekel HG, Metters AT, Weber FE, Fields GB, et al. Synthetic matrix metalloproteinase-sensitive hydrogels for the conduction of tissue regeneration: engineering cell-invasion characteristics. *Proc Natl Acad Sci USA* 2003;100:5413–8. [PubMed: 12686696]
7. Seliktar D, Zisch AH, Lutolf MP, Wrana JL, Hubbell JA. MMP-2 sensitive, VEGF-bearing bioactive hydrogels for promotion of vascular healing. *J Biomed Mater Res A* 2004;68:704–16. [PubMed: 14986325]
8. Dikovskiy D, Bianco-Peled H, Seliktar D. The effect of structural alterations of PEG-fibrinogen hydrogel scaffolds on 3-D cellular morphology and cellular migration. *Biomaterials* 2006;27:1496–506. [PubMed: 16243393]
9. Benoit D, Schwartz M, Durney A, Anseth K. Small functional groups for controlled differentiation of hydrogel-encapsulated human mesenchymal stem cells. *Nat Mater* 2008;7:816–23. [PubMed: 18724374]
10. Fairbanks B, Scott T, Kloxin C, Anseth K, Bowman C. Thiol Yne Photopolymerizations: Novel Mechanism, Kinetics, and Step-Growth Formation of Highly Cross-Linked Networks. *Macromolecules* 2009;42:211–7. [PubMed: 19461871]
11. Gobin AS, West JL. Cell migration through defined, synthetic ECM analogs. *FASEB J* 2002;16:751–3. [PubMed: 11923220]
12. Lee S-H, Moon JJ, Miller JS, West JL. Poly(ethylene glycol) hydrogels conjugated with a collagenase-sensitive fluorogenic substrate to visualize collagenase activity during three-dimensional cell migration. *Biomaterials* 2007;28:3163–70. [PubMed: 17395258]

13. Raeber GP, Lutolf MP, Hubbell JA. Mechanisms of 3-D migration and matrix remodeling of fibroblasts within artificial ECMs. *Acta Biomater* 2007;3:615–29. [PubMed: 17572164]
14. Elisseeff J, Anseth K, Sims D, McIntosh W, Randolph M, Yaremchuk M, et al. Transdermal photopolymerization of poly(ethylene oxide)-based injectable hydrogels for tissue-engineered cartilage. *Plast Reconstr Surg* 1999;104:1014–22. [PubMed: 10654741]
15. Lee HJ, Lee J-S, Chansakul T, Yu C, Elisseeff JH, Yu SM. Collagen mimetic peptide-conjugated photopolymerizable PEG hydrogel. *Biomaterials* 2006;27:5268–76. [PubMed: 16797067]
16. Liu Tsang V, Chen AA, Cho LM, Jadin KD, Sah RL, DeLong S, et al. Fabrication of 3D hepatic tissues by additive photopatterning of cellular hydrogels. *FASEB J* 2007;21:790–801. [PubMed: 17197384]
17. Shah DN, Recktenwall-Work SM, Anseth KS. The effect of bioactive hydrogels on the secretion of extracellular matrix molecules by valvular interstitial cells. *Biomaterials* 2008;29:2060–72. [PubMed: 18237775]
18. Lutolf MP, Weber FE, Schmoekel HG, Schense JC, Kohler T, Müller R, et al. Repair of bone defects using synthetic mimetics of collagenous extracellular matrices. *Nat Biotechnol* 2003;21:513–8. [PubMed: 12704396]
19. Mapili G, Lu Y, Chen S, Roy K. Laser-layered microfabrication of spatially patterned functionalized tissue-engineering scaffolds. *J Biomed Mater Res B Appl Biomater* 2005;75:414–24. [PubMed: 16025464]
20. Hahn MS, McHale MK, Wang E, Schmedlen RH, West JL. Physiologic pulsatile flow bioreactor conditioning of poly(ethylene glycol)-based tissue engineered vascular grafts. *Ann Biomed Eng* 2007;35:190–200. [PubMed: 17180465]
21. Mann BK, Gobin AS, Tsai AT, Schmedlen RH, West JL. Smooth muscle cell growth in photopolymerized hydrogels with cell adhesive and proteolytically degradable domains: synthetic ECM analogs for tissue engineering. *Biomaterials* 2001;22:3045–51. [PubMed: 11575479]
22. Aimetti AA, Machen AJ, Anseth KS. Poly(ethylene glycol) hydrogels formed by thiol-ene photopolymerization for enzyme-responsive protein delivery. *Biomaterials* 2009;30:6048–54. [PubMed: 19674784]
23. DeForest CA, Polizzotti BD, Anseth KS. Sequential click reactions for synthesizing and patterning three-dimensional cell microenvironments. *Nat Mater* 2009;8:659–64. [PubMed: 19543279]
24. Krishnan L, Underwood CJ, Maas S, Ellis BJ, Kode TC, Hoying JB, et al. Effect of mechanical boundary conditions on orientation of angiogenic microvessels. *Cardiovasc Res* 2008;78:324–32. [PubMed: 18310100]
25. Staton CA, Reed MWR, Brown NJ. A critical analysis of current in vitro and in vivo angiogenesis assays. *Int J Exp Pathol* 2009;90:195–221. [PubMed: 19563606]
26. Mammoto A, Connor KM, Mammoto T, Yung CW, Huh D, Aderman CM, et al. A mechanosensitive transcriptional mechanism that controls angiogenesis. *Nature* 2009;457:1103–8. [PubMed: 19242469]
27. Zisch AH, Lutolf MP, Ehrbar M, Raeber GP, Rizzi SC, Davies N, et al. Cell-demanded release of VEGF from synthetic, biointeractive cell ingrowth matrices for vascularized tissue growth. *FASEB J* 2003;17:2260–2. [PubMed: 14563693]
28. Ehrbar M, Rizzi SC, Hlushchuk R, Djonov V, Zisch AH, Hubbell JA, et al. Enzymatic formation of modular cell-instructive fibrin analogs for tissue engineering. *Biomaterials* 2007;28:3856–66. [PubMed: 17568666]
29. Leslie-Barbick JE, Moon JJ, West JL. Covalently-immobilized vascular endothelial growth factor promotes endothelial cell tubulogenesis in poly(ethylene glycol) diacrylate hydrogels. *J Biomater Sci Polym Ed* 2009;20:1763–79. [PubMed: 19723440]
30. Moon JJ, Lee S-H, West JL. Synthetic biomimetic hydrogels incorporated with ephrin-A1 for therapeutic angiogenesis. *Biomacromolecules* 2007;8:42–9. [PubMed: 17206786]
31. Imper, V.; Van Wart, HE. Substrate Specificity and Mechanisms of Substrate Recognition of the Matrix Metalloproteinases. In: Parks, WC.; Mecham, RP., editors. A chapter in *Matrix Metalloproteinases*. Academic Press; 1998. p. 219–42.

32. Lee S-H, Miller JS, Moon JJ, West JL. Proteolytically degradable hydrogels with a fluorogenic substrate for studies of cellular proteolytic activity and migration. *Biotechnol Prog* 2005;21:1736–41. [PubMed: 16321059]
33. Lowry OH, Rosebrough NJ, Farr AL, Randall RJ. Protein measurement with the Folin phenol reagent. *J Biol Chem* 1951;193:265–75. [PubMed: 14907713]
34. Moon JJ, Hahn MS, Kim I, Nsiah BA, West JL. Micropatterning of poly(ethylene glycol) diacrylate hydrogels with biomolecules to regulate and guide endothelial morphogenesis. *Tissue Eng Part A* 2009;15:579–85. [PubMed: 18803481]
35. Auerbach R, Lewis R, Shinnars B, Kubai L, Akhtar N. Angiogenesis assays: a critical overview. *Clin Chem* 2003;49:32–40. [PubMed: 12507958]
36. Aplin AC, Fogel E, Zorzi P, Nicosia RF. The aortic ring model of angiogenesis. *Meth Enzymol* 2008;443:119–36. [PubMed: 18772014]
37. Adams RH, Alitalo K. Molecular regulation of angiogenesis and lymphangiogenesis. *Nat Rev Mol Cell Biol* 2007;8:464–78. [PubMed: 17522591]
38. Chun T-H, Sabeh F, Ota I, Murphy H, McDonagh KT, Holmbeck K, et al. MT1-MMP-dependent neovessel formation within the confines of the three-dimensional extracellular matrix. *J Cell Biol* 2004;167:757–67. [PubMed: 15545316]
39. Ghajar CM, George SC, Putnam AJ. Matrix metalloproteinase control of capillary morphogenesis. *Crit Rev Eukaryot Gene Expr* 2008;18:251–78. [PubMed: 18540825]
40. Jilani SM, Murphy TJ, Thai SNM, Eichmann A, Alva JA, Iruela-Arispe ML. Selective binding of lectins to embryonic chicken vasculature. *J Histochem Cytochem* 2003;51:597–604. [PubMed: 12704207]

**Figure 1.**

(a) Synthetic scheme. PEG 3400 is reacted with acryloyl chloride to form PEGDA, which is then reacted with cysteine-bearing peptides via Michael-type addition to form cell-adhesive or, in a separate reaction, MMP-sensitive PEG-acrylate macromers. Reaction stoichiometry controls the molecular weight and polydispersity of the resultant species during step-growth polymerization. (b) Schematic illustration of hydrogel structure. Photopolymerization of the photoactive precursors from (a) yields bioactive hydrogels with multiple MMP-sensitive peptides per backbone chain, with pendant cell-adhesive ligands tethered from sites of acrylate crosslinking.

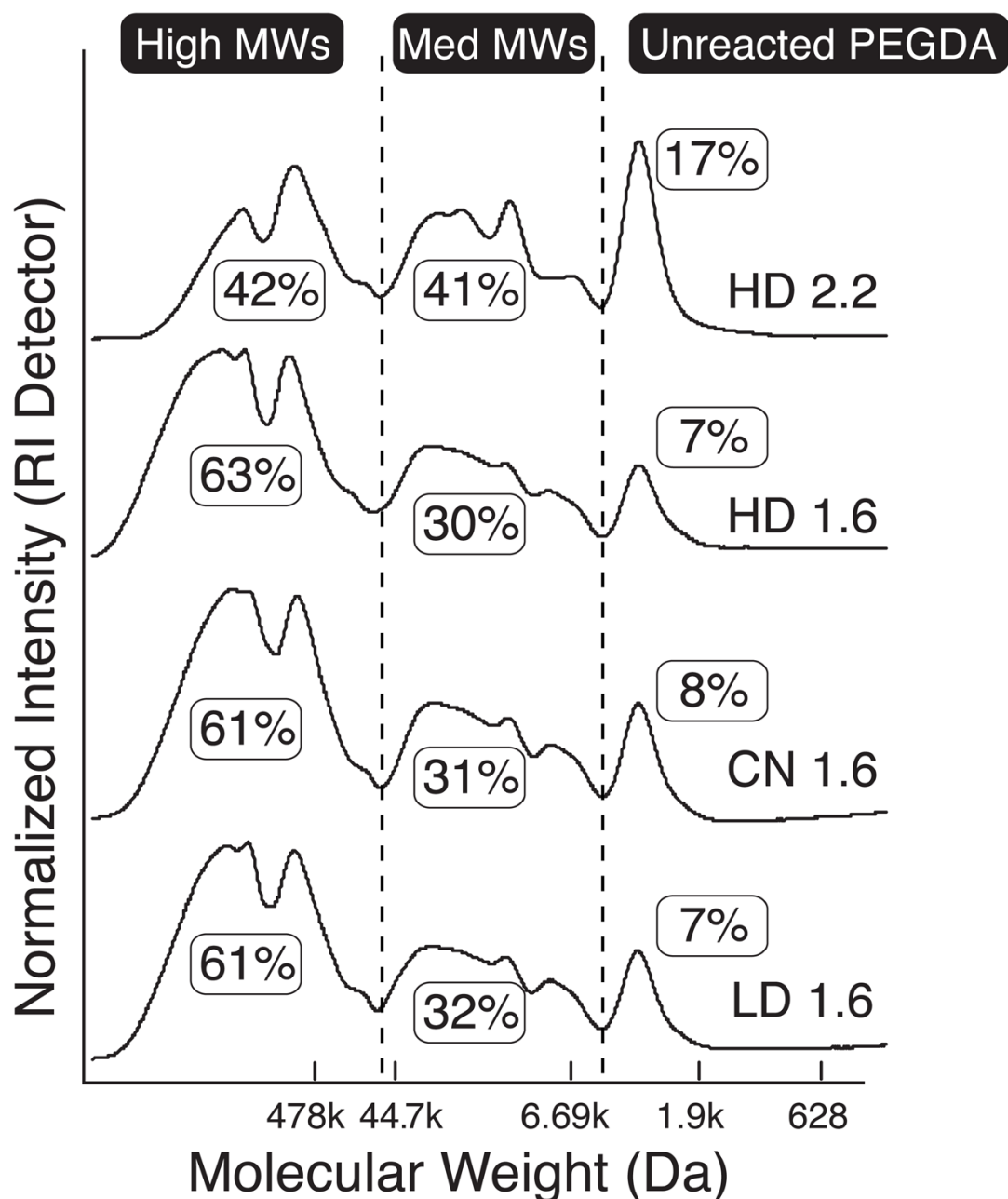
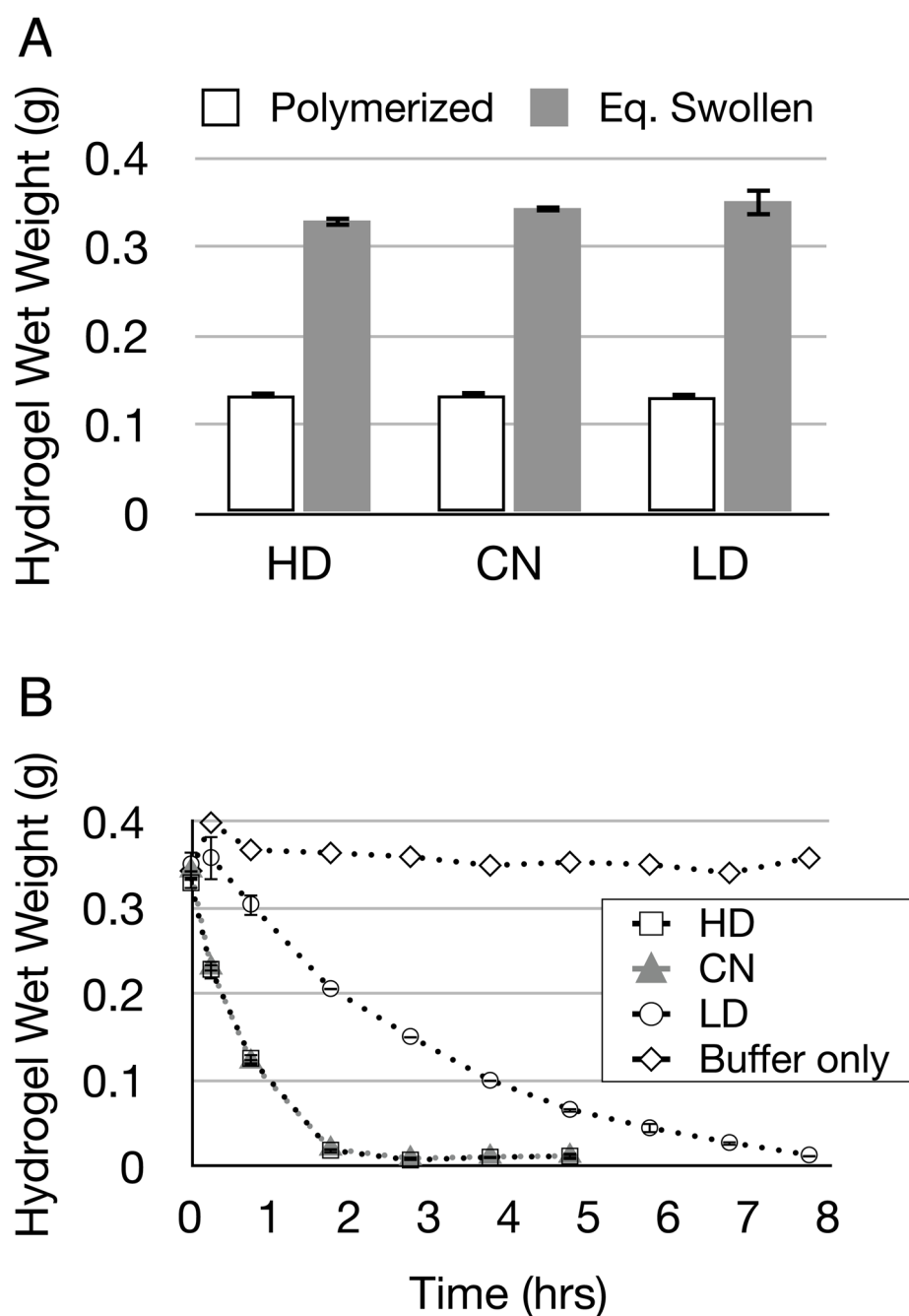
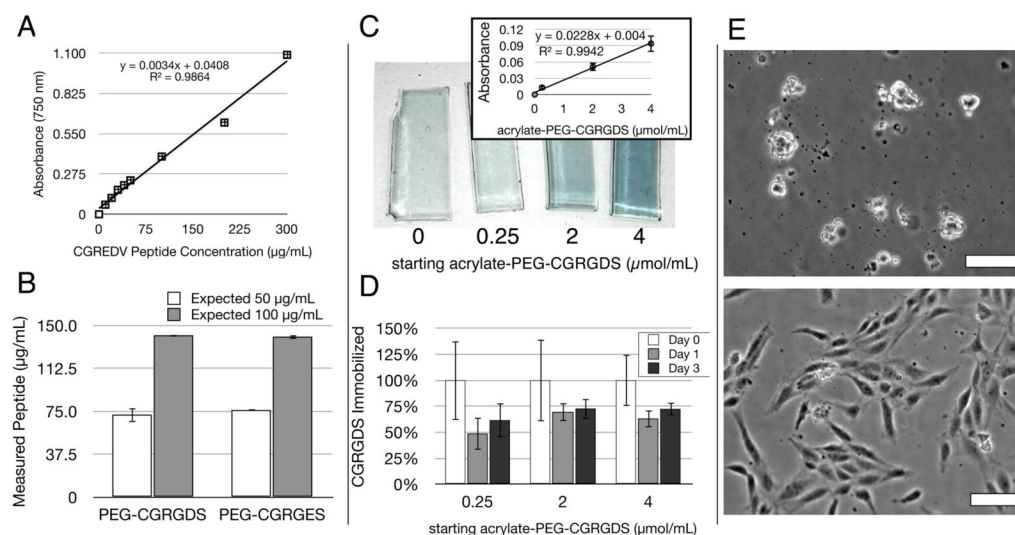


Figure 2.

GPC analysis of MMP-sensitive PEG-diacrylates plotted against PEG MW standards. Highly degradable (“HD”) peptide reacted with a 2.2 molar excess of PEGDA (uppermost curve) via step-growth polymerization resulted in more than 80% conjugation (sum of Medium and High MWs). Reaction of MMP-sensitive peptides with a 1.6 molar excess of PEGDA (remaining three curves) resulted in more than 90% conjugation, with a majority of the molecular weight species greater than 500 kDa. When subjected to the same reaction stoichiometry, HD, collagen native (“CN”), and least degradable (“LD”) PEG-peptide conjugates show nearly identical polydispersity.

**Figure 3.**

(a) MMP-sensitive hydrogels (made from HD, CN, or LD peptides) were polymerized at 10% w/w and then swollen to equilibrium over 36 hours (n=3, Eq. Swollen in figure). Bars indicate standard deviation. (b) Swollen hydrogels were degraded in 0.2 mg/mL collagenase (n=3) or incubated in buffer (n=1) up to 8 hours while their wet weight was monitored. Note that HD and CN have overlapping degradation curves. Bars indicate standard deviation.

**Figure 4.**

The immobilization efficiency and stability of acrylate-PEG-peptide macromers in PEGDA gels was assessed with a modified Lowry Assay for total protein concentration, as well as HUVEC seeding. **(a)** The Lowry assay, typically only used for large proteins, produced a linear standard curve from the short, soluble CGREDV peptide, even at low concentrations. **(b)** This standard curve was used to quantify the solution-based concentration of acrylate-PEG-CGRGDS and acrylate-PEG-CGRGES macromers, with a deviation from expected of 40–50%, with values comparable between both peptides. Bars indicate standard error. **(c)** gross appearance of hydrogel slabs after modified Lowry Assay *in situ* showing characteristic blue color with starting peptide concentration (μmol/mL). The linear dependence on concentration was also valid in solid hydrogels (inset, bars indicate standard deviation). **(d)** The assay tracked CGRGDS retention over time within hydrogels. A large percent of RGDS was lost on the first day during hydrogel equilibrium swelling. The remaining peptide was stable for at least 2 more days in the gel (n=3 for all samples), with up to 75% retention. Bars indicate standard deviation. **(e)** HUVEC morphology on PEGDA hydrogels with 4.0 μmol/mL PEG-CGRGES (**top**) or PEG-CGRGDS (**bottom**) 24 hours post-seeding. Scale Bars = 25 μm.

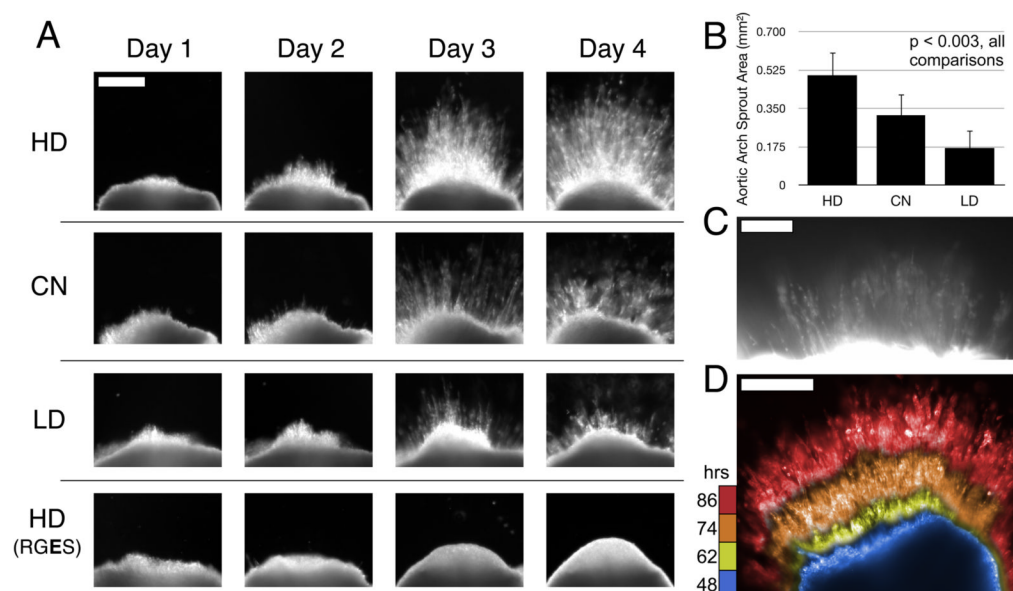


Figure 5.

(a) Representative images of chick aortic arch ring explants sprouting into hydrogels over time. In 8-wt% gels with 1.0 $\mu\text{mol/mL}$ CGRGDS density, angiogenic sprouting varies with the MMP-susceptibility of the hydrogel backbone. No detectable sprouting occurred in negative control hydrogels containing RGES instead of RGDS peptide. Scale bar for all images = 250 μm . (b) Quantification of sprout area at Day 4, $n=6$ per condition. Mean with standard deviation, all comparisons are significant, $p < 0.003$ by one-way ANOVA and Tukey's HSD post-hoc testing. (c) Fluorescent staining with lectin-rhodamine implicates endothelial cells as a principal component of the angiogenic sprouts in these hydrogels. Scale Bar = 100 μm . (d) Composite image of selected frames during sprouting time-course by dark field imaging (see supplemental Movie 1), false colored then overlaid here to aid in time visualization. Blue, yellow, orange, red = 48, 62, 74, 86 hours respectively. Scale Bar = 250 μm .